Water Research 170 (2020) 115301

Contents lists available at ScienceDirect

Water Research

journal homepage: www.elsevier.com/locate/watres

How water isotopes (^{18}O, ^{2}H, ^{3}H) within an island freshwater lens respond to changes in rainfall

Eliza Bryan [a, b, c], Karina T. Meredith [a, b, *], Andy Baker [b, c], Martin S. Andersen [b, d], Vincent E.A. Post [e], Pauline C. Treble [a, b]

[a] Australian Nuclear Science and Technology Organisation, Lucas Heights, NSW, 2234, Australia
[b] Connected Waters Initiative Research Centre, UNSW Sydney, NSW, 2052, Australia
[c] School of Biological Earth and Environmental Sciences, UNSW Sydney, NSW, 2052, Australia
[d] School of Civil and Environmental Engineering, UNSW Sydney, NSW, 2052, Australia
[e] College of Science and Engineering and National Centre for Groundwater Research and Training, Flinders University, Adelaide, Australia

ARTICLE INFO

Article history:
Received 20 May 2019
Received in revised form
3 November 2019
Accepted 9 November 2019
Available online 11 November 2019

Keywords:
Island freshwater lens
Water isotopes
Seawater intrusion
Mean groundwater residence time

ABSTRACT

Coastal aquifers provide an important source of water globally. Understanding how groundwater responds to changes in rainfall recharge is important for sustainable development. To this end, we investigate how water isotopes (^{18}O, ^{2}H, ^{3}H) and chloride (Cl) concentrations within an island freshwater lens respond under varying rainfall conditions in a region experiencing climate change. Uniquely, this study presents a three year dataset of groundwater collected seasonally between May 2013 and August 2016 from ten wells. Variation in all tracers was observed. The Cl and tritium (^{3}H) show opposing seasonal variation in some sections of the lens, with higher Cl observed in the austral summer when less rainfall occurs and evapotranspiration is highest. The opposite occurs in the austral winter months when ^{3}H increases from atmospheric input via rainfall recharge, and Cl is diluted. An overall decline in ^{3}H values and enrichment in stable water isotopes over the study period was also observed. This study shows that understanding groundwater of freshwater lenses should not rely on a single sampling campaign because seasonal variability is large. The identification of a dual recharge regime, with contributions from both winter rainfall and episodic events, has important implications for understanding the future fate of the freshwater lens on Rottnest Island. The finding that episodic rainfall is a major contributor to groundwater recharge is important and can only be assessed with a multi-year isotope dataset for groundwater and rainfall.

1. Introduction

Coastal aquifers provide a source of water for more than one billion people (Small and Nicholls, 2003) and are under increasing strain due to rapid population growth in coastal areas globally. These aquifers come with various challenges when utilised as a potable water source, including seawater intrusion caused by both natural and anthropogenic causes (Kinzelbach et al., 2003; Post, 2005; Barlow and Reichard, 2010; Jiao and Post. 2019). While groundwater abstraction is one of the leading causes of seawater intrusion, the impacts of climate change on coastal aquifers is also of concern (Ferguson and Gleeson, 2012). Global sea level rise (SLR) promotes seawater intrusion (Nicholls et al., 2007), but perhaps more importantly, a decline in recharge in areas of reduced rainfall leads to a subsequent decrease in the volume of freshwater available for utilisation (White and Falkland, 2010). These issues can be intensified on islands, where fresh groundwater is usually present in the form of a shallow lens 'floating' on more saline water below due to the density difference. These lenses are particularly vulnerable to climate variability, as their very existence relies on rainfall recharge (White and Falkland, 2010).

Understanding how rainfall recharges freshwater lenses and determining the residence time of groundwater are therefore particularly important. Tritium (^{3}H) and helium have been previously used, typically based on the Vogel (1967) method, to estimate recharge to freshwater lenses (Houben et al., 2014; Röper et al., 2012). Vogel (1967) developed an analytical model to calculate

* Corresponding author. Australian Nuclear Science and Technology Organisation, Lucas Heights, NSW, 2234, Australia.
E-mail address: karina.meredith@ansto.gov.au (K.T. Meredith).

https://doi.org/10.1016/j.watres.2019.115301

the age stratification of groundwater over a vertical profile, assuming an evenly recharged, homogeneous aquifer of constant depth with horizontal flow. However in a seasonally dynamic system, estimating recharge patterns and groundwater residence times requires a more comprehensive approach such as incorporating water isotopes including ^{3}H time-series. Time-series data of stable water isotopes have been used previously by Jones and Banner (2003) in the tropical islands Barbados, Guam and Puerto Rico to determine the timing of recharge events. This approach was not useful on Bermuda where there was no distinct seasonality of rainfall δ^{18}O. In New Caledonia on the other hand, Nicolini et al. (2016) established that there was a seasonal variation of rainfall δ^{18}O, but groundwater δ^{18}O was found to be essentially constant over time, which the authors attributed to a combination of two processes; a large threshold of 120–140 mm of monthly rainfall for recharge to occur, and the mixing of rainfall in the soil zone with waters from previous events that have been influenced by evapotranspiration. Similarly, Beal et al. (2019) recently inferred a bias towards high-rainfall periods during the wet season based on δ^{18}O values in groundwater and cave drip water in Guam. Recharge was found to be sensitive to inter-annual variations in rainfall amount and intensity, highlighting the sensitivity of island freshwater lenses to seasonal or yearly climate variability. Röper et al. (2012) investigated groundwater age distribution, recharge conditions and hydrochemistry of a barrier island freshwater lens in the southern North Sea using ^{3}H–^{3}He ages and stable water isotopes based on two sample events. This study had a limited number of groundwater ages ($n = 9$) but they found young waters in the shallow sections of the lens (12 m) increasing in age to greater than 70 years at the fresh-water-saltwater interface (Röper et al., 2012). Houben et al. (2014) showed that a freshwater lens on the northern German island of Langeoog contains climate information reflecting environmental conditions at the time of recharge.

The knowledge on how current climate change scenarios will impact groundwater resources remains limited (Cartwright and Simmonds, 2008) but recently Cuthbert et al. (2019) suggested that groundwater systems may respond to long-term (e.g. decadal) responses based on modelling. Rottnest Island, located off the coast of Perth, Australia, provides a unique setting to investigate the effect of rainfall decline over the past few decades on groundwater contained in a freshwater lens. Since 1965, south-west Western Australia has undergone a ~20% decline in mean winter precipitation. The rainfall decline has been attributed to a reorganisation in the southern hemisphere circulation systems, particularly the south-eastern Indian Ocean atmospheric and oceanic circulation (Evans et al., 2009; Smith et al., 2000) and a strong positive phase of the southern annular mode. The decline in rainfall has affected the region's storage and management of water resources, with a study investigating the freshwater lens on Rottnest Island finding this has had a considerable impact on the extent of the groundwater resource (Bryan et al., 2016). Historical rainfall records and groundwater abstraction rates showed that the shrinkage of the freshwater lens was found to be primarily caused by a decrease in rainfall, which led to the contraction in the lens (1 km^{2} seen in Fig. 1A; Bryan et al., 2016), leading to seawater intrusion, with both modern (<50 years) and old (~3–7 ka) seawater being present in the aquifer (Bryan et al., 2017).

The objective of this study is to investigate whether long-term climate change (decadal to centennial) or short-term seasonal changes in rainfall are influencing the isotopic character of a shallow (0–30 m) freshwater lens on Rottnest Island. Previous studies have investigated the extent of seawater mixing, calculated groundwater residence times and assessed the long-term rainfall (decadal) and groundwater abstraction patterns for the island. However, these assessments were based on one or two sample events (Bryan et al., 2016; Bryan et al., 2017), which most groundwater chemistry investigations generally are. While these datasets are informative, they do not allow the assessment of variations over time. Therefore, this study presents a seasonal groundwater isotopic and Cl dataset collected over a three year period (May 2013 to August 2016) This study is unique in that we present groundwater data collected from the two field campaigns described in Bryan et al. (2016) and Bryan et al. (2017) together with three years of seasonal groundwater monitoring data, and compare it with rainfall data collected to evaluate how the freshwater lens responds to rainfall recharge. Specifically, this study uses environmental tracers (Cl, ^{2}H, ^{18}O and ^{3}H) to evaluate the recharge mechanisms (winter vs. episodic events), residence times and the interaction of the transition zone within a fresh water lens. This is the first study to use seasonal isotopic groundwater data to provide insights on the impacts of the reduction in rainfall and how it is influencing the fresh water lens for this region. The outcomes of this study are expected to provide a useful guide for understanding how fresh water lenses on islands respond to changes in seasonal rainfall regimes.

2. Study area

Rottnest Island is located approximately 18 km off the coast of Perth in south-west Western Australia (Fig. 1A) and is ~10.5 km long and up to 4.5 km wide, with a maximum elevation of ~45 m above Australian Height Datum (AHD). Rottnest Island has a Mediterranean type climate characterised by hot, dry summers and mild, wet winters, with 80% of annual precipitation falling between May and September. Weather systems impacting on the region are dominated by anti-cyclonic high-pressure systems with periodic tropic and mid-latitude depressions and local seasonal sea-breezes (Eliot and Clarke, 1986). While the island has a long term average rainfall of 688 mm/year (1880–2016), the south-west Western Australian region has experienced a decrease in rainfall since the mid 1960's and a particular decline since 2000 (Bates et al., 2008), with average rainfall decreasing at the study site over time: 746 ± 154 (1880–1965), 608 ± 118 (1966–1999) and 556 ± 112 (2000–2016) mm. Annual rainfall in each year of the study period, especially 2014, was below the long-term average (2013 = 632 mm, 2014 = 487 mm, 2015 = 543 mm, 2016 = 612 mm). The island's land-use and vegetation history have been described in detail in Bryan et al. (2016). Some parts of the island have recently been revegetated, however the area above the freshwater lens has generally been left free of large trees to maximise recharge to the freshwater lens.

2.1. Hydrogeological setting

The hydrogeological setting has been summarised by Bryan et al. (2016) and Bryan et al. (2017). Briefly, the island is composed of Pleistocene to mid-Holocene carbonate aeolianite (Tamala Limestone) with a total thickness of ~115 m (Playford and Leech, 1977). The Tamala Limestone consists of creamy-white to yellow, or light-grey calcarenites which contains various proportions of quartz sand, fine-to medium-grained shell fragments, and minor clayey lenses (Playford et al., 1976). It is composed of 50–99% fine to coarse sand-sized carbonate bioclasts (Hearty and O'Leary, 2008; Mory, 1995; Playford, 1997; Playford et al., 1976) and is strongly lithified to friable. There are no fresh surface water features due to the highly permeable nature of the Tamala Limestone but there are hypersaline lakes on the eastern side of the island.

The transition zone below the fresh groundwater is reported to be more than 10 m thick (Edward and Watson, 1959; Playford and Leech, 1977). The water table was previously measured to be at a

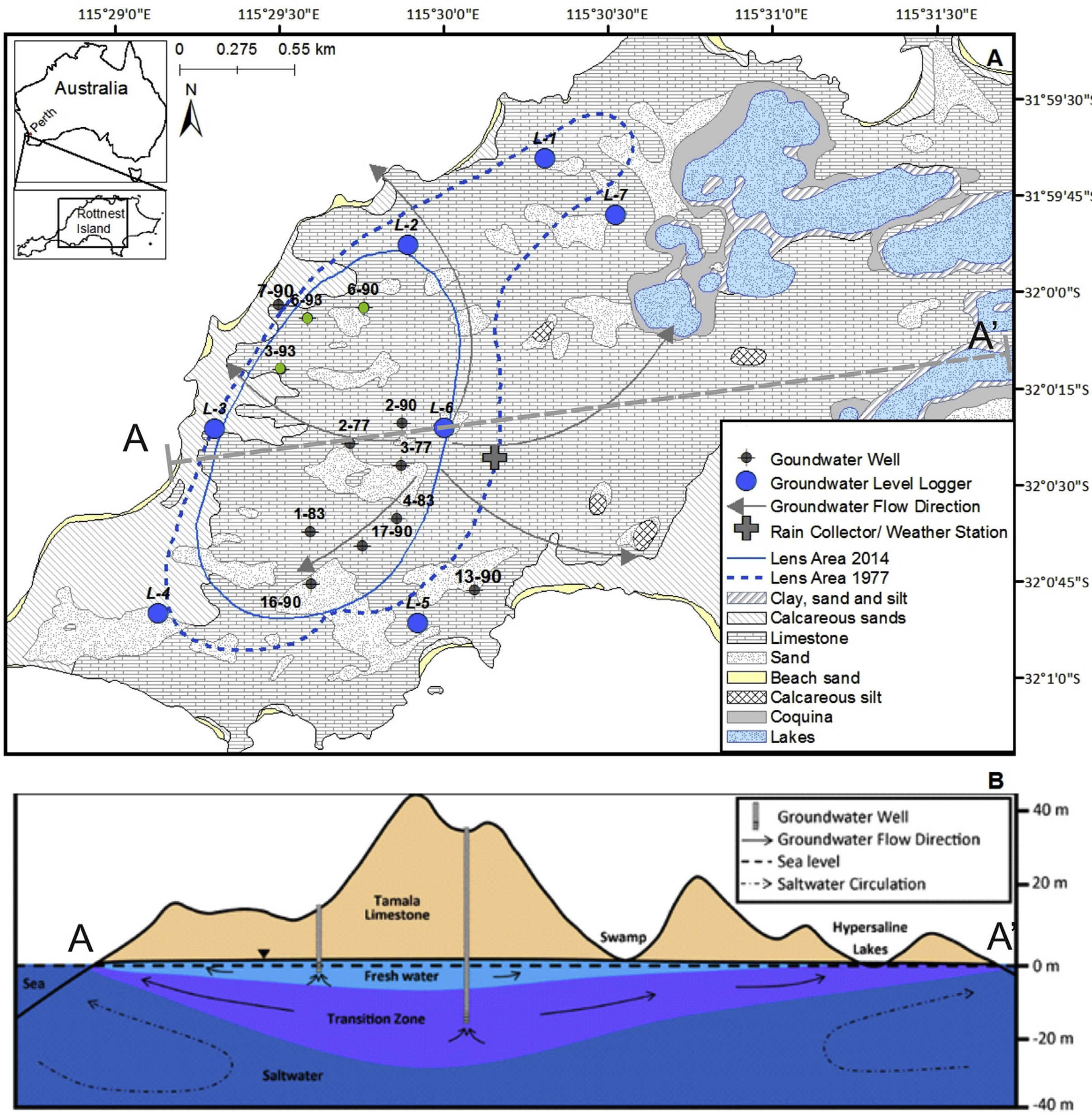

Fig. 1. A) Location and geological map of the study area showing sample and water logger locations, weather station and rainfall collector location. Grey arrows represent the generalised groundwater flow direction based on Sept 2014 water level data. Grey dashed line A-A′ represents the location of the cross section. Green dots represent wells in Figs. 3 and 4. Lens area is represented for 1977 and 2014; and B) a simplified east-west cross section of Rottnest Island (A-A′), adapted from Smith (1985), showing groundwater flow directions and the circulation of seawater which is induced by the mixing of freshwater and saltwater in the mixing zone. (For interpretation of the references to colour in this figure legend, the reader is referred to the Web version of this article.)

maximum of ~0.5 m above sea level, with groundwater flowing from the centre of the lens towards the coast and hypersaline lakes (Bryan et al., 2016). The spatial extent of the freshwater lens has contracted significantly (1 km^2) since the late 1970s due to a ~20% decline in precipitation since the mid-1960s (Fig. 1A) (Bryan et al., 2016). The aquifer has been used as a potable water source since the 1970s, with the volume of abstraction in recent years between 5 and 9% of rainfall recharge (Bryan et al., 2016). The groundwater abstraction wells are very shallow and tap the top of the water table, with 1 mlong well screens ranging from −0.6 to 0.1 m AHD. Groundwater abstraction has occurred historically from the lens where up to 120,000 m^3 per year was used for public water supply on the island. The volume has been reduced significantly over the years resulting in the cessation of pumping in 2018. In 2014, groundwater abstraction had reduced to 17% of the volume of previous years (~21,400 m^3) (Bryan et al., 2016).

3. Methods

During twelve field campaigns between May 2013 and August 2016, 110 samples were collected from production wells throughout the study area (Fig. 1A). The sample collection and analysis procedure has been described previously (Bryan et al. 2016, 2017). In brief, samples were collected using permanently installed pumps after purging until stabilisation of in-field parameters including pH, temperature, electrical conductivity (EC) and dissolved oxygen (DO). Composite rainfall samples were collected on a weekly basis from June 2013 to December 2016 in a rainfall collector designed to collect samples for isotopic analysis by preventing evaporation. The Cl and isotopic (δ^{18}O, δ^{2}H, ^{3}H) analysis of groundwaters and rainfall was carried out according to the methodology presented by Bryan et al. (2016). The Cl concentration of water samples were analysed by ion chromatography. The δ^{18}O and δ^{2}H were analysed by isotope ratio mass spectrometry (IRMS) and values were reported as per mil (‰) deviation from the international standard V-SMOW2 (Vienna Standard Mean Ocean Water). The δ^{18}O samples were analysed using an equilibration, continuous flow IRMS method while δ^{2}H samples were analysed using an on-line combustion, dual-inlet IRMS method. The δ^{18}O and δ^{2}H measurements were reproducible to ±0.15‰ and ±1‰, respectively. The ^{3}H samples were analysed, with water samples being distilled and electrolytically enriched prior to analysis by a liquid scintillation method. The ^{3}H concentrations were expressed in tritium units (TU) with a general uncertainty of ±0.1 TU and quantification limit of 0.06 TU.

Water levels were monitored at 30 min increments at a subset of monitoring wells for over 2 years from September 2014 to December 2016 using non-vented Solinst Gold Loggers which were corrected for barometric pressure. Hydrographs were constructed from the 2014–2016 dataset using an adjacent averaging method to highlight the general trends in water levels over time (Fig. 2A).

Groundwater age distributions were evaluated using TracerLPM (Jurgens et al., 2012). This modelling package permits optimization of parameters using either multiple tracers analysed in a single sample (Tracer-Tracer method) or from a single tracer analysed in multiple samples collected over a period of time (Time-Series method) (Jurgens et al., 2012). A detailed description of the commonly used lumped parameter models (LMPs) is discussed in Jurgens et al. (2012) and Maloszewski et al. (2002). Briefly, LMPs are mathematical models of transport based on aquifer geometry and flow that accounts for hydrodynamic dispersion or mixing within the aquifer, discharge area or the well (Jurgens et al., 2012). Testing and selection of an appropriate LPM for an aquifer system is needed because the mean age is often non-unique between the models. The LPM approach assumes tracers are injected and travel conservatively with the water molecule through the aquifer. Therefore, the mean age inferred by tracer concentrations is equal to the mean age of water discharging from the system or to a screened interval (Jurgens et al., 2012). LPMs were used in this study for groundwater residence time calculations because they account for the age distribution of the sample.

All individual LMPs (piston-flow model, exponential mixing model, exponential piston-flow model, partial exponential model, and dispersion model) were assessed including binary mixing models, which have been previously used to describe tracer concentrations in karstic aquifers and watersheds with variations in

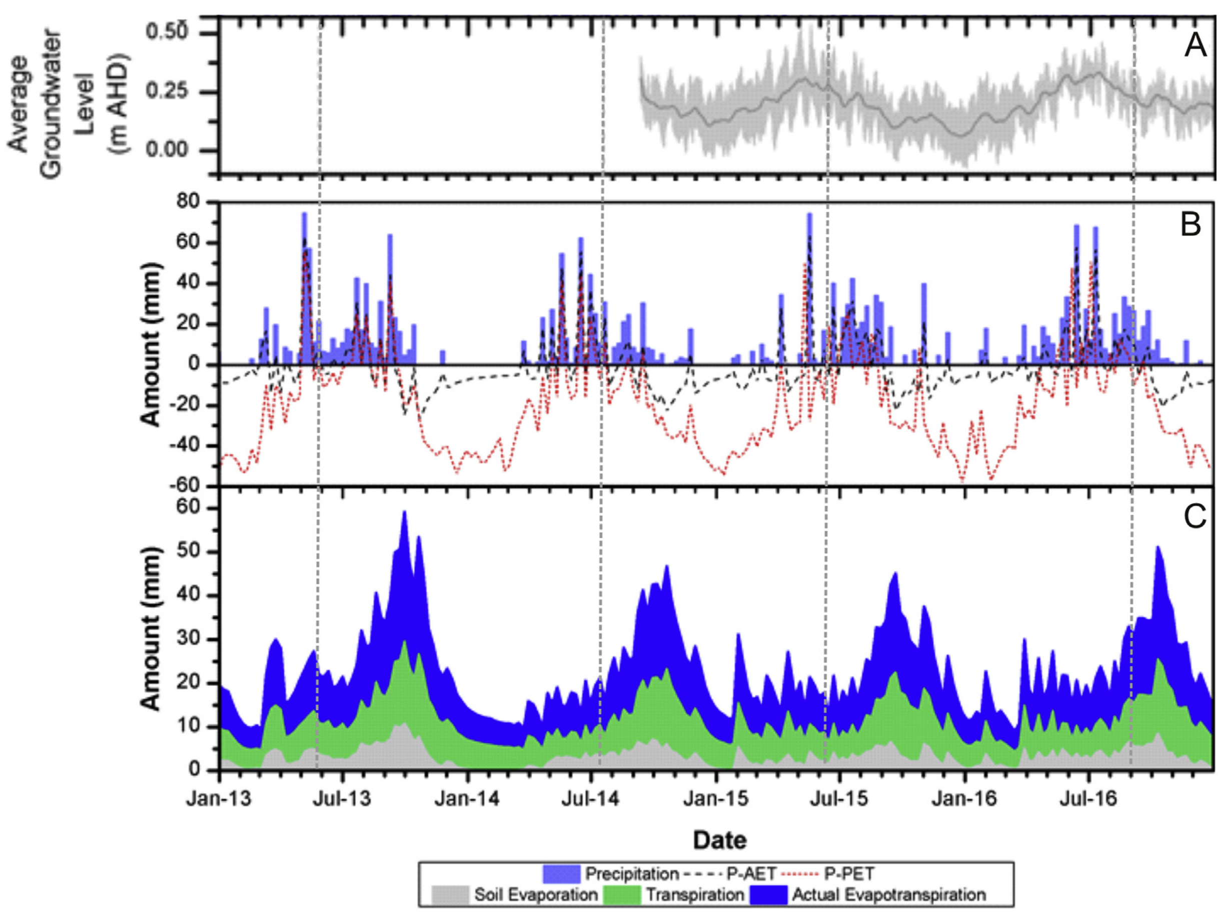

Fig. 2. (A) Average (smoothed) groundwater level (solid line) (see text for description) and standard deviation (shaded area) (between September 2014 and December 2016 only), B) Weekly rainfall amount, weekly rainfall totals (P) modelled actual evapotranspiration (AET) and P-actual evapotranspiration (PET) and C) Australian Water Availability Project (AWAP) modelled values for AET, soil evaporation and transpiration over the monitoring period. Methodology for construction of Figures is provided in section 3. The vertical grey dashed lines indicate periods when recharge was observed.

transmissivity (Jurgens et al., 2012; Katz et al., 2009; Long and Putnam, 2006). The models were run for five wells (6–90, 3–77, 4–83, 1–83 and 16–90) where time-series ^3H data was collected over the study period. The tracers ^3H and ^{18}O were used in combination and then separately for each model.

The ^3H and ^{18}O monthly rainfall from 1962 to 2020 are used as input data to the model. The ^3H input data was from the ^3H in rainfall measured by the Global Network of Isotope in Precipitation (GNIP) and ANSTO on a monthly basis since the 1960s at Perth, Western Australia, which is in close proximity (<50 km) to the study site. Pre-bomb atmospheric concentrations and atmospheric concentrations, since November 2016 (when rainfall data was no longer available) were assumed to be 2 TU. Where data was absent, ^3H values were estimated by interpolation. An ^{18}O input function was also used, with Perth rainfall ^{18}O values from GNIP (IAEA/WMO, 2016) utilised where available. Where data was absent, a monthly average value was calculated based on existing data. Values for $\delta^{18}O$ in groundwater were also included in the modelling because they are a useful model constraint for rainfall recharge in the LMPs. The ^{18}O rainfall time series were constructed from data from the nearby GNIP monitoring station at Perth, supplemented by data collected as part of this study from Rottnest Island from 2014 to 2016. Missing data and data prior to GNIP monitoring was interpolated based on the monthly mean.

Composite rainfall samples were collected on Rottnest Island on a weekly basis from May 2014 in a rainfall collector designed to collect samples for isotopic analysis by preventing evaporation. Besides rainfall data, we utilise modelled climate parameters for the study site location from the Australian Water Availability Project (AWAP) dataset (Raupach et al., 2009, 2012). Modelled AWAP weekly climate parameters from nineteen sites around Perth, WA, were used to calculate average values that were subsequently utilised in calculations for Rottnest Island, as the AWAP model domain does not extend to Rottnest Island (Fig. 2B and C). A cumulative water budget was calculated using Bureau of meteorology rainfall (BOM, 2017) and modelled actual evapotranspiration (AET) data to obtain the total recharge to the freshwater lens for each year of the study (2013–2016). Weekly modelled AET is subtracted from weekly rainfall totals (P) to determine the water budget (i.e. P − AET). Potential recharge is then calculated from all positive monthly water budgets (monthly excess rainfall). The total sum of all monthly excess water for each year gives the potential infiltration for that particular year.

4. Results

Groundwater levels were measured from dedicated monitoring wells as indicated in Fig. 1A and were responsive to tidal oscillations causing large daily fluctuations. The average filtered groundwater levels reveal the seasonal trends better (Fig. 2A). All locations showing the same characteristic water level fluctuations over time, which appear to be heavily dependent on rainfall and a return to near sea level during low rainfall periods (Fig. 2B): The highest water levels are observed in the austral winter months (~0.5 m above mean sea level) which are characterised by high rainfall, while lower water levels (near 0 m AHD) are observed in the austral summer months (Fig. 2B). The wells sampled for this study were production wells used to abstract groundwater. It was found that the decrease in rainfall since the 1970s had a greater influence on water levels than groundwater abstraction volume (Bryan et al., 2016).

The annual mean actual evapotranspiration (AET) for Rottnest Island using the Australian Water Availability Project (AWAP) dataset is 615 ± 57 mm, with soil evaporation and transpiration accounting for 171 ± 29 mm and 444 ± 30 mm, respectively (Raupach et al., 2009, 2012). An average annual potential recharge of 280 ± 10 mm during the study period was calculated using rainfall and modelled AET data, ranging from a minimum of 265 mm in 2014 to a maximum of 295 mm in 2015, which are consistent with previously calculated recharge estimates of between 147 and 245 mm per year calculated using the renewal rate calculation with ^3H as the rainfall input and groundwater age tracer (Bryan et al., 2016).

4.1. Environmental tracers

The average rainfall Cl concentration over the study period is 1.9 ± 1.8 mmol/L, while average groundwater Cl concentrations range from 4.5 ± 0.7 to 9.1 ± 4.3 mmol/L (Table 1). Groundwater Cl concentrations range between 4.0 and 20.0 mmol/L (with a smaller range detected in most wells) (Fig. 3B). Higher Cl values were measured in the austral summer and early autumn months, when limited rainfall occurs, with average groundwater Cl concentrations ranging from 7.8 ± 2.6 to 9.1 ± 4.3 mmol/L (Table 1, Fig. 3B). Average groundwater Cl values in the higher-rainfall austral winter months range from 4.8 ± 0.8 to 5.2 ± 1.1 mmol/L. Moreover, greater variability is observed in the austral summer months, while less

Table 1
Summary of hydrochemistry and isotopic data of rainfall and fresh groundwaters from production wells.

Date	Cl			δ^2H			$\delta^{18}O$			d-excess			^3H		
	Av.[a]	SD[b]	n	Av.	SD	n	Av.	SD	n	Av.	SD	n	Av.	SD	n
	mmol/L	mmol/L		‰	‰		‰	‰		‰	‰		TU	TU	
May-13	4.5	0.7	9	−17.7	1.3	9	−3.9	0.4	9	13.6	1.8	9	1.16	0.29	8
Oct-13	5.2	0.7	10	−18.4	1.4	10	−4.1	0.2	10	14.7	0.8	10	0.97	0.17	10
Mar-14	9.1	2.6	10	−17.8	0.9	10	−4.1	0.2	10	14.8	0.9	10	0.88	0.16	5
Jul-14	5.2	0.8	10	−17.9	1.1	10	−4.1	0.2	10	15.2	0.8	10	0.96	0.17	5
Sep-14	5.6	1.1	10	−18.4	1.1	10	−4.1	0.2	10	14.7	1.3	10	0.87	0.16	10
Jan-15	7.9	4.3	9	−17.7	1.0	9	−4.1	0.2	9	15.1	0.8	9	0.81	0.19	4
Mar-15	8.8	4.1	10	−18.2	0.9	10	−4.2	0.2	10	15.5	0.5	10	0.74	0.20	5
Jun-15	4.8	1.1	7	−17.4	1.3	7	−4.1	0.3	7	15.3	0.9	7	0.88	0.15	2
Sep-15	5.0	1.3	9	−17.5	1.2	9	−4.0	0.2	9	14.9	0.9	9	0.88	0.12	4
Jan-16	7.8	2.8	8	−17.7	1.0	8	−4.1	0.2	8	15.1	0.8	8	0.83	0.17	4
Mar-16	8.3	3.9	10	−16.6	0.9	10	−3.9	0.2	10	15.0	0.8	10	0.77	0.15	5
Aug-16	4.8	0.8	8	−16.7	1.1	9	−4.0	0.2	9	14.9	0.9	8	0.89	0.10	8
Rainfall	1.9	1.8	92	−17.7	1.3	98	−3.9	0.4	98	14.7	4.5	98	1.78[c]	0.63[c]	33[c]

[a] Average.
[b] Standard Deviation.
[c] Unpublished ANSTO data and IAEA/WMO (2016).

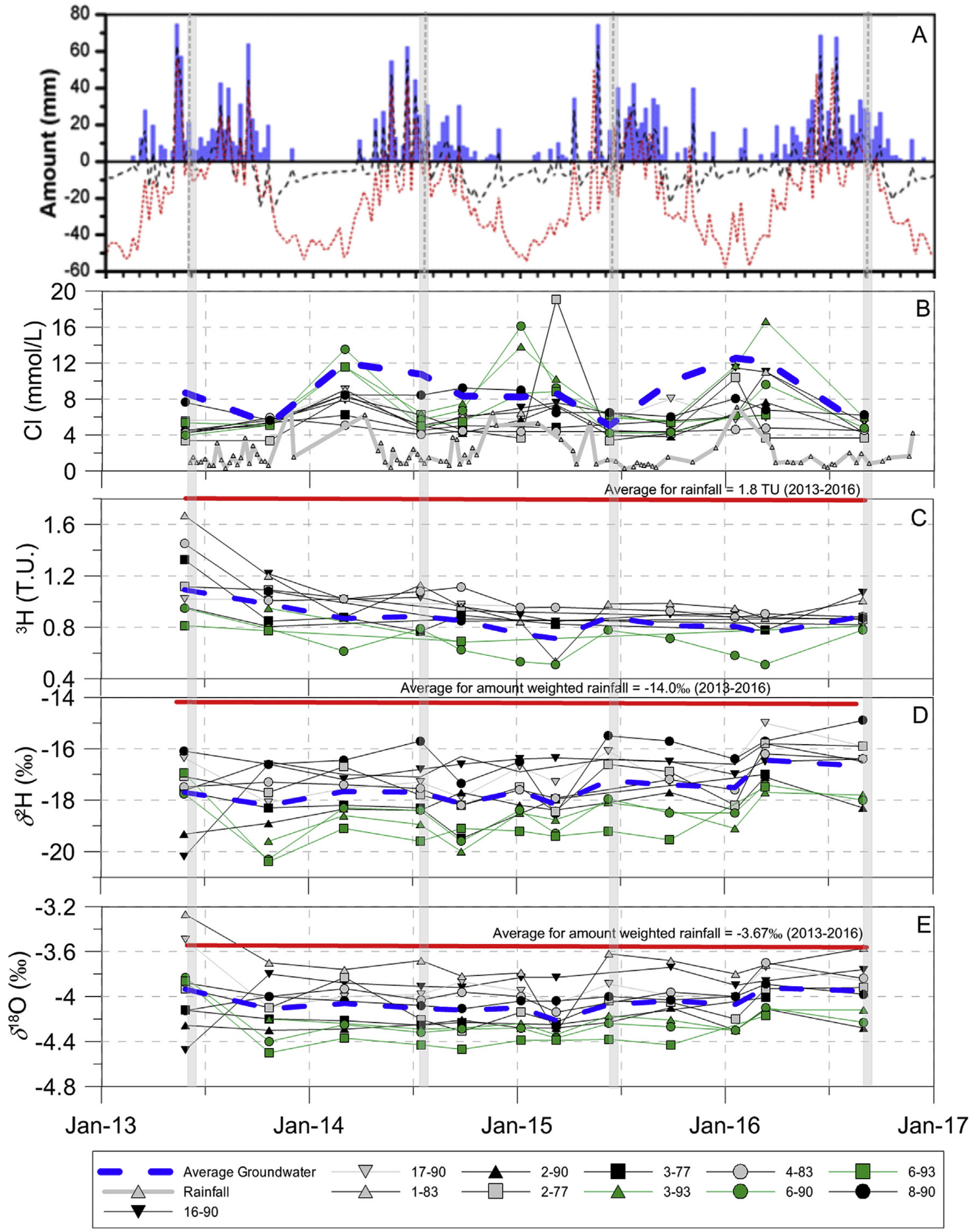

Fig. 3. Timeseries over the study period between January 2013 and December 2016: A) Weekly rainfall amount, P-AET and P-PET (ref to Fig. 2 for description) B) Rainfall Cl concentration and Groundwater Cl concentration, C) Groundwater ^{3}H compared to average rainfall ^{3}H over 2013–2016, D) Groundwater δ^{2}H compared to amount weighted average rainfall δ^{2}H over 2013–2016 and E) Groundwater δ^{18}O compared to amount weighted average rainfall δ^{18}O over 2013–2016. Green lines indicate wells in the NW region of the lens (Fig. 1).
The blue dashed line represents the average concentration for the tracer. The vertical grey opaque lines indicate periods when recharge was observed. (For interpretation of the references to colour in this figure legend, the reader is referred to the Web version of this article.)

variability is observed in the austral winter months (Fig. 3B). The data for most wells follow a similar temporal pattern, however for some wells a slightly earlier or later peak in Cl concentrations during the austral summer months is observed (Fig. 3B). During the summer of 2013/14, very little rain fell and the Cl peaks for all groundwaters were aligned. In the subsequent two summers on the other hand, some summer rainfall occurred and variation in the timing of the Cl peaks was observed. Three wells which show repeated, higher increases in Cl concentration (6–90, 3–93 and 6–93) during the austral summer are located in the north-west

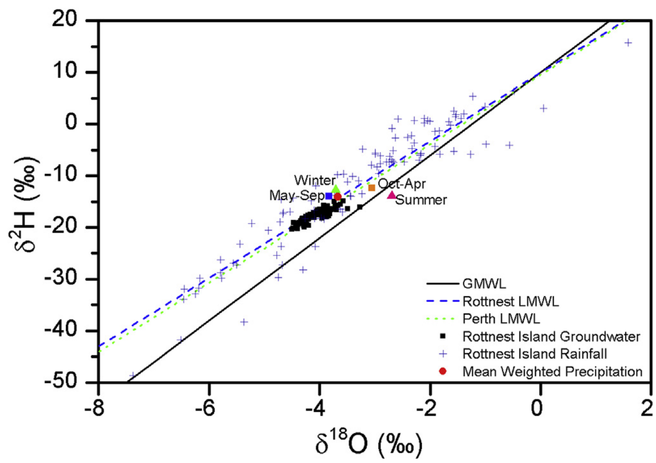

Fig. 4. A bivariate plot depicting δ^2H vs. δ^{18}O for groundwaters and rainfall from the study site, as well as the Global Meteoric Water Line (GMWL; $\delta^2H = 8*\delta^{18}O+10$), the Perth Local Meteoric Water Line (LMWL; $\delta^2H = 6.7*\delta^{18}O+9.5$) and the Rottnest Island LMWL ($\delta^2H = 6.6*\delta^{18}O+9.9$), with mean weighted precipitation results for winter and summer.

(NW) area of the freshwater lens and are represented in green in Fig. 3B. With a significant Cl peak in March 2016, well 2–77, located towards the centre of the lens (Fig. 1A) with a very shallow well screen (−0.49 m AHD), deviates from all other wells (Fig. 3B).

The average ^{3}H value of Perth rainfall over the study period between May 2013 and August 2016 was 1.78 ± 0.63 TU (Table 1; unpublished ANSTO data and IAEA/WMO (2016)). Average groundwater ^{3}H concentrations over the same period range from 0.74 ± 0.10 to 1.16 ± 0.29 TU. While average ^{3}H values show an overall decline over the study period (Fig. 3C), ^{3}H values rise slightly during the austral winter months, before decreasing slowly until the next winter. The five wells that were monitored on a regular basis show varying fluctuations over time and some wells show opposing patterns between Cl and ^{3}H values. The opposite relationship was most notable in groundwaters with a higher concentration of Cl (e.g. well 6–90) (Table S1). The greatest proportion of recharge from rainfall occurs in the austral winter months, which corresponds to when groundwaters have higher average ^{3}H values compared to other times throughout the year (Fig. 3C, blue line). The highest ^{3}H groundwater values however, were observed in May 2013 (Fig. 3C), averaging 1.16 ± 0.29 TU.

Rainfall values for δ^2H and δ^{18}O ranged from −48.7 to 15.7‰ and from −7.4 to 1.6‰ respectively between May 2013 and July 2016. Based on rainfall δ^{18}O and δ^2H values, a Local Meteoric Water Line (LMWL) for Rottnest Island was calculated using a precipitation weighted least squares regression method (Crawford et al., 2014), which is given by $\delta^2H = 6.6*\delta^{18}O+9.9$ (Fig. 4). The Rottnest Island LMWL lies right beside the LMWL for the Perth Region, given by $\delta^2H = 6.7*\delta^{18}O+9.5$ (Hollins et al., 2018, Fig. 4), which was expected due to their close proximity. Average groundwater δ^2H values range from −18.2 to −16.4‰ (Fig. 3D; Table 1) over the study period, while average groundwater δ^{18}O values range from −4.2 to −3.9‰ (Fig. 3E). The groundwater data points lie on the Rottnest LMWL, which suggests a rainfall origin and that waters have not been significantly influenced by evaporation prior to recharge (Fig. 4). The mean weighted precipitation isotope composition over the study period (δ^{18}O: 3.67‰; δ^2H: 14.09‰) is more positive than most groundwater samples (Fig. 4). While average δ^{18}O and δ^2H groundwater values are fairly constant throughout the study period, there does appear to be a very slight upward trend in δ^2H values as indicated with the average groundwater line in blue (Fig. 3D).

4.2. Groundwater residence times

The ^{3}H values in shallow groundwaters (4–20 m below ground surface) on Rottnest Island vary significantly, which is an important finding when considering most groundwater age assessments use ^{3}H from one sampling event. As a result, the most accurate way to use the ^{3}H values to calculate groundwater residence times is to use a LPM, as it takes into consideration the source ^{3}H fluctuations and allows for the determination of more accurate mean residence times. The determination of an LPM from a single tracer, such as tritium, measured in a single sample is non-unique (Jurgens et al., 2012). The reason for this is tritium has an input history concentration change over time. As a result, measured tritium concentrations can correspond to more than one mean age.

The LPM results show that a combination of ^{3}H and ^{18}O tracers are required to achieve a good model fit at the study site (Table 2 and Table S2), with the use of ^{3}H and ^{18}O individually resulting in significantly higher model errors (as high as −441% average error; Table 2) compared to when both tracers are used (whereby errors were generally < 10%). The mean residence time values from the combined tracer models are used in this study. The binary mixing

Table 2
A summary of mean residence time results in years. All results can be found in Table S2.

Well ID	Tracer	Min.[a] Age	Max.[b] Age	Average Age	Min. Error	Max. Error	Average Error
1–83	^{3}H	27.07	84.68	49.18	151%	229%	187%
	^{18}O	10.00	55.96	36.36	−621%	−131%	−348%
	^{3}H, ^{18}O	15.00	61.56	40.85	−1%	81%	25%
16–90	^{3}H	31.60	75.69	41.45	68%	132%	86%
	^{18}O	7.80	44.80	28.79	−519%	−136%	−302%
	^{3}H, ^{18}O	12.00	64.00	39.38	−5%	4%	0%
4–83	^{3}H	22.34	78.79	51.71	56%	173%	104%
	^{18}O	10.00	63.88	39.82	−580%	−174%	−362%
	^{3}H, ^{18}O	11.50	52.42	37.45	−3%	8%	1%
6–90	^{3}H	28.60	91.37	71.45	103%	294%	170%
	^{18}O	0.00	63.88	34.86	−590%	−317%	−441%
	^{3}H, ^{18}O	26.90	63.64	53.33	−2%	17%	3%
3–77	^{3}H	27.22	68.57	48.01	32%	78%	53%
	^{18}O	0.00	44.80	27.15	−392%	−151%	−263%
	^{3}H, ^{18}O	17.80	64.85	44.80	−7%	4%	0%

[a] Minimum.
[b] Maximum.

models were expected to be superior over the single lumped parameter models due to the karstic nature of the Tamala Limestone. However, the single dispersion models produced consistently lower errors compared to the binary mixing models (Table S2) and this may be due to the young eogenetic limestones on Rottnest Island, which have limited karstification and therefore exhibit porous media behaviour. The dispersion model likely addresses the dual flow properties of the karst, and the modelled residence times provide a ‘mean’ age, which will be a mixture of both younger and older waters. The limited role of karsification is supported by the relatively young ages of the Tamala Limestone formation (Hearty, 2003; Lipar and Webb, 2014).

The mean residence times from all dual tracer models range from a minimum of ~12 years to a maximum of ~65 years (Table 2, Table S2). Overall, the dispersion model (DM) performs most consistently (in terms of error) across all sites for the dual tracers with more consistent mean residence times (range: 12–36 years) and low errors regularly achieved across each site (−0.8 to 3.8%). Most fresh groundwater samples from the lens were calculated to have mean residence times between 12 and 18 years. This indicates groundwaters were recharged over the most recent period of rainfall decline experienced for south-west Western Australia. However samples in the NW of the lens (well 6–90, Table S2) were calculated to have double the mean residence time (36 years) of wells sampled in other areas of the lens (Fig. 5).

5. Discussion

5.1. Seasonal changes

The temporal groundwater data appears to indicate that increasing AET and low rainfall produce higher Cl concentrations in groundwater, which coincide with low water levels and decrease in ^{3}H values in some wells. Although Rottnest Island has a high potential for evaporation, we see no direct evidence of evaporation in the δ^2H and δ^{18}O values for the groundwater, rather they closely resemble rainfall plotting close to the LWML (Fig. 4). In fact, four recharge pulses can be identified during the monitoring period, as inferred from decreases in Cl concentration in groundwater, coinciding with periods of rainfall with low Cl content and higher winter rainfall amounts prior to sampling. The seasonal change in the Cl concentration suggests that rainfall recharge dilutes the groundwater.

Transpiration results in the increase of Cl concentrations in the soil water or groundwater without ^{18}O-enrichment in the root zone (Farquhar et al., 2007). This would explain the observation in our dataset because we do not see enrichment in δ^2H and δ^{18}O values. This has also been observed in the Tamala Limestone on the mainland of Australia (Treble et al., 2016), whereby the Cl concentrations in cave drip waters were affected by transpiration, and the drip water did not show isotopic enrichment associated with evaporation. The modelled AWAP data shows that transpiration on Rottnest Island accounts for up to 60% of AET (Fig. 2C). This means that direct evaporation is also significant, which would leave an imprint on the isotopic signature unless the evaporation is complete. Smaller rainfall events are susceptible to direct evaporation as they are not transmitted into the deeper parts of the soil as rapidly as high-intensity rainfall events. Complete evaporation of these small rainfall amounts does indeed fit with the observed bias of the groundwater towards rainfall with a depleted isotopic composition, which is associated with the more intense rainfall events.

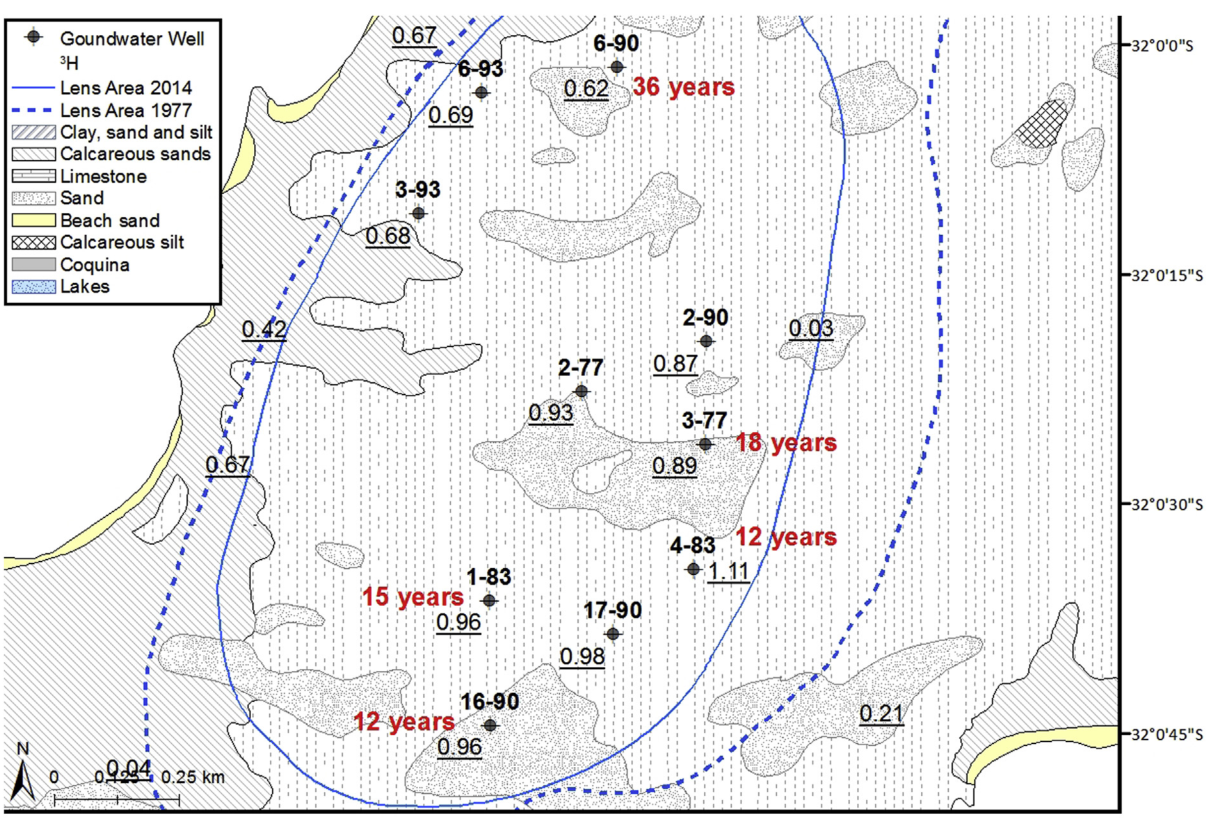

Fig. 5. Map of ^{3}H content (underlined numbers in TU) after Sept 2014 sample event (Bryan et al., 2016) with mean residence times (indicated in red) rounded to the nearest year calculated from this study. Lens areas are represented for 1977 and 2014 (Bryan et al., 2016). (For interpretation of the references to colour in this figure legend, the reader is referred to the Web version of this article.)

The Cl concentration in the groundwater increased after periods with a P-AET deficit (Fig. 3) during the austral summer. Besides the dry summer of 2013/2014, when no variation in the timing of Cl peaks in groundwaters were observed, sporadic rainfall over the late spring and summer of 2014/15 and 2015/16 would allow for the flushing of Cl concentrated by evapotranspiration in the unsaturated zone down to the water table, which would subsequently increase the groundwater Cl concentration. Similarly, the complete evaporation of water from low-intensity rainfall events that do not reach the water table and the remaining salts being flushed down by subsequent high intensity events would also produce an increase in Cl with no enrichment in water isotopes. Furthermore, the leaching of Cl accumulated on the vegetation by dry deposition of airborne sea salts may further contribute to a rise of the groundwater Cl concentration following the earliest rainfall after a dry period (Bresciani et al., 2014). These Cl accumulation mechanisms provide an explanation for the variation in Cl peaks (Fig. 3B).

Three of the four recharge events were not large enough to change the groundwater ^{3}H values to the rainfall highs that were observed in May 2013 (Fig. 3C). One reason might be that subsequent recharge events had lower ^{3}H rainfall values, but there is no evidence for this in the rainfall ^{3}H record. An explanation for the lower ^{3}H values for the recharge events could be that the sampled groundwater becomes mixed with deeper older groundwater from various parts of the lens and that the rainfall amount over the three years was not large enough to displace the older groundwater in the sampled zones. This fits with other studies of island freshwater lenses that found groundwaters increased in age to greater than 70 years at the fresh-water-saltwater interface (Röper et al., 2012). It was also found by Maloszewski et al. (2002) by using ^{18}O and ^{3}H as tracers that transit times are monthly in comparison with the mean transit times of decades through a fissured-porous aquifer.

5.2. Transition zone mixing

An alternative explanation for why we see elevated Cl and lower ^{3}H values in the fresh water lens could be the change in location of the transition zone between summer and winter. The most significant Cl variations are found in the wells located closest to the coast in the NW area of the lens (wells 6–90, 3–93 and 6–93; green lines in Fig. 3B) and are located in relatively close proximity (150–400 m) to well 7–90 which is affected by seawater intrusion as described elsewhere (Bryan et al. 2016, 2017).

Yet the δ^{18}O and δ^2H values of groundwaters from these wells do not show clear evidence of seawater mixing. This can be explained because the maximum possible seawater proportion was calculated to be between 0.2 and 2.0% of the total volume of water, therefore, this minor amount of seawater would not affect the δ^{18}O isotopic value of the groundwater by more than ~0.1‰ (2% of a signal with 0‰ compared to 98% of a signal with −4.0‰), which is within the measurement error.

Therefore the seasonal Cl variation for the NW wells (6–90, 3–93 and 6–93) could be the vertical movement of the transition zone. This would lead to Cl being transported upwards with deeper saline groundwater in summer due to the reduction in rainfall recharge which leads to a contraction of the thickness of the freshwater lens. We do not have the data to prove conclusively whether the observed groundwater Cl variations are driven primarily by unsaturated zone processes or the movement of the lens boundary with upward dispersion of Cl from the transition zone. However, we have assessed that the possible impact from the latter on the mean residence time calculations to be insignificant because the less than 2% seawater contribution represents an uncertainty too small to be noted in the stable isotope analysis. Likewise, it would only contribute a maximum of 2% of older ^{3}H depleted transition zone water. The potential error introduced in the model by a portion of older water from below is therefore small and constrained to the NW area of the lens.

Considering the high transmissivity of the limestone, it is expected that the lens volume will respond to the perturbations in recharge and sea level. Contraction of the freshwater lens during late summer when groundwater levels are lowest will occur because groundwater constantly discharges to the sea, negligible rainfall recharge occurs and, albeit to a small extent, groundwater is withdrawn by pumping. The rising water table due to rainfall recharge and cessation of pumping in winter will restore the lens volume. The fresh-saltwater interface thus moves up and down in response to the seasonality of the rainfall, as has been shown for carbonate aquifers elsewhere (Post et al., 2018). The drop in groundwater levels by the end of summer causes older, ^{3}H depleted, groundwater with higher concentrations of Cl to migrate upwards, with the reverse occurring in the winter months when recharge occurs, and provides an explanation for the observed inverse relationship between Cl and ^{3}H in many of the wells in the NW region.

5.3. Episodic recharge

Temporal variations in the dataset suggest various rainfall patterns are governing the observed seasonal trends in the data. The May 2013 sampling campaign occurred after the wettest May on record in eight years in Perth resulting from a low pressure system comprised of multiple cold fronts (BOM, 2013). Approximately 140 mm of rainfall was recorded in the 20 days prior, with a large rainfall event comprised of 61 mm falling in 24 h on the 8th May, 2013 (20 days before), and a further 10.5 mm falling in the following 24-hour period. Clear indications for recharge to the lens are provided by groundwater samples containing ^{3}H (May 2013 average groundwater $^3\mathrm{H} = 1.16 \pm 0.29$ TU), similar to the rainfall for that month (1.24 TU) (unpublished ANSTO data and IAEA/WMO (2016)) (Table S1). This event appeared to affect the entire system demonstrating the importance of episodic recharge by large rainfall events for the lens. Indeed some wells (1–83, 3–77 and 4–83) had higher groundwater values than the rainfall input value (Table S1) suggesting the episodic recharge event had higher ^{3}H contents than the monthly weighted average of rainfall. The δ^{18}O values of the groundwater are also lower than the mean δ^{18}O value of winter precipitation (Fig. 3E), again supporting the suggestion that episodic rainfall events (that have a lighter isotopic signature) contribute to recharge, as well as the regular winter rains. Combined with the observation that LPM modelling of the ^{18}O tracer (Perth monthly rainfall) resulted in δ^{18}O values more positive than the observed groundwater δ^{18}O data, causing a consistent negative model fit (Table 2), the results show that such episodic events may be more important than seasonal winter recharge in maintaining the volume of the fresh water lens.

This assessment is supported by the study undertaken by Barron et al. (2012) who found that for most climates in Australia the correlation between recharge and the annual rainfall parameters reflecting rainfall intensity were stronger than the correlation between modelled recharge and total annual rainfall. Furthermore, studies in the Golgotha cave in the Tamala limestone on the mainland found that cave drip rates, which are indicative of recharge, remained almost constant for a period of several years (Mahmud et al., 2016; Treble et al. 2013, 2016) despite highly seasonal winter precipitation and a summer soil moisture deficit. As on Rottnest Island, the May 2013 recharge event had a strong impact on the hydrology of the limestone of the Golgotha cave, with drip rates abruptly increasing after years of near-constancy (Mahmud et al., 2016).

5.4. Implications for future recharge

The finding from this study that episodic rainfall is a major contributor to groundwater recharge from winter rainfall is important and this assessment would not be possible without seasonal time-series data. This is because under climate projections of decreased *total* rainfall for the region (Crosbie et al., 2012; Ng et al., 2010), recharge may be sustained if the frequency of *high-intensity rainfall* events were to increase. Significantly the groundwater recharged over the past few decades with mean residence times ranging from 12 to 36 years occurred during the ongoing lower than average rainfall periods experienced in the south-west Western Australia region. This leads to questions about the impact of recharge variations, with future predictions of rainfall from global climate models suggesting that the region could see further declines in winter rainfall by approximately 40% from the 1911–1970 average (Delworth and Zeng, 2014). Several factors are expected to contribute to the change in climate, including an enhancement of atmospheric surface pressure over parts of Australia, which are consistent with a southerly shift and intensification of the subtropical ridge and the Hadley cell (Delworth and Zeng, 2014). The modelled rainfall decline is also affected by the long-term increasing trend in the southern annular mode which results in a southerly shift of westerly winds and rain-producing storms (Delworth and Zeng, 2014) producing a further reduction in winter rainfall. This is likely to affect recharge to the freshwater lens which in turn will affect the extent of the fresh groundwater store at the study site.

Further investigations are required to deduce the impact of soil moisture conditions on recharge. Nagra et al. (2017) determined a recharge threshold value of about 90 mm for the Tamala Limestone on the mainland, which emphasises the importance of large storm events like the May 2013 recharge event on Rottnest Island. The occurrence of such large recharge events is infrequent in south-west Western Australia, and further investigations are required to determine the effect that climate change may have on both their frequency and intensity, and on the resulting recharge potential. Ongoing monitoring of the freshwater lens into the future is thus essential to determine if the continued decrease in rainfall for the region is reflected by changes in the aquifer, which is important for both the management of this resource, and other shallow, unconfined aquifers globally.

6. Conclusions

The objective of this study was to investigate whether long-term climate variability (decadal) or short-term seasonal changes in rainfall were influencing the isotopic character of a freshwater lens on Rottnest Island. The study was undertaken during a period of lower than average rainfall for the region (May 2013 to August 2016). A large rainfall event in May 2013 allowed us to evaluate winter season vs. episodic recharge mechanisms. It was found that two key processes can result in the seasonal variation observed. Primarily the processes were reliant on the location of the monitoring wells within the lens. In the centre of the lens, the Cl and ^{3}H variations were governed by the seasonal variation, for example increased Cl and lower ^{3}H during the summer months were driven by higher evapotranspiration and lower rainfall. The groundwater residence times in this part of the aquifer range from 12 to 18 years. In the NW section of the lens, the shrinkage and upward movement of the freshwater lens when the water table falls in summeris possible.

The results from this study highlighted the importance of a time-series approach including multiple parameters for monitoring shallow, unconfined aquifers, to have sufficient input data to drive a process-based model (e.g. lumped parameter model), and to ensure that seasonal variability is captured. Groundwater studies of freshwater lenses should not rely on a single sampling campaign because this study shows the seasonal variability is large. The ^{3}H values in shallow aquifers can vary considerably over a study period, for example the greatest observed ^{3}H variation in a single groundwater well ranged from 0.54 TU to 1.67 TU. This observation is important for using ^{3}H as a dating and modelling tool.

Groundwater Cl concentrations were indicative of recharge processes highlighting the importance of evapotranspiration, while ^{3}H was important for the deduction of the long-term recharge trends, and also illustrates the importance of large episodic rainfall events. The identification of a dual recharge regime, with contributions from both winter rainfall and episodic events, has important implications for understanding the future fate of the freshwater lens.

Declaration of competing interest

The authors declare that they have no known competing financial interests or personal relationships that could have appeared to influence the work reported in this paper.

Acknowledgements

This research was partially funded by an Australian Research Council Linkage Project LP150100144 to AB and KM, supported by partners ANSTO, Rottnest Island Authority, ANU and the WA Department of Water. EB was supported by an Australian Government Research Training Program postgraduate award. Groundwater loggers were funded by the National Collaborative Research Infrastructure Strategy (NCRIS). We would like to acknowledge the support of ANSTO's laboratory staff and RIA support staff. EB and KM were responsible for the majority of the fieldwork, supported by AB, MSA and VP. EB was responsible for all laboratory analyses and writing of the manuscript, to which all authors contributed.

Appendix A. Supplementary data

Supplementary data to this article can be found online at https://doi.org/10.1016/j.watres.2019.115301.

References

Barlow, P.M., Reichard, E.G., 2010. Saltwater intrusion in coastal regions of North America. Hydrogeol. J. 18 (1), 247–260.
Barron, O., Crosbie, R., Dawes, W., Charles, S., Pickett, T., Donn, M., 2012. Climatic controls on diffuse groundwater recharge across Australia. Hydrol. Earth Syst. Sci. 16 (12), 4557–4570.
Bates, B.C., Hope, P., Ryan, B., Smith, I., Charles, S., 2008. Key findings from the Indian Ocean Climate Initiative and their impact on policy development in Australia. Clim. Change 89 (3), 339–354.
Beal, L.K., Wong, C.I., Bautista, K.K., Jenson, J.W., Banner, J.L., Lander, M.A., Gingerich, S.B., Partin, J.W., Hardt, B., van Oort, N.H., 2019. Isotopic and geochemical assessment of the sensitivity of groundwater resources of Guam, Mariana Islands, to intra- and inter-annual variations in hydroclimate. J. Hydrol. 568, 174–183.
BOM, 2013. Perth in May 2013: Wettest May for Eight Years. Bureau of Meteorology, Australian Government.
BOM, 2017. Evapotranspiration Calculations. Bureau of Meterology, Australian Government.
Bresciani, E., Ordens, C.M., Werner, A.D., Batelaan, O., Guan, H., Post, V.E.A., 2014. Spatial variability of chloride deposition in a vegetated coastal area: implications for groundwater recharge estimation. J. Hydrol. 519, 1177–1191.
Bryan, E., Meredith, K.T., Baker, A., Andersen, M.S., Post, V.E.A., 2017. Carbon dynamics in a Late Quaternary-age coastal limestone aquifer system undergoing saltwater intrusion. Sci. Total Environ. 607–608, 771–785.
Bryan, E., Meredith, K.T., Baker, A., Post, V.E.A., Andersen, M.S., 2016. Island groundwater resources, impacts of abstraction and a drying climate: Rottnest Island, Western Australia. J. Hydrol. 542, 704–718.
Cartwright, I., Simmonds, I., 2008. Impact of changing climate and land use on the

hydrogeology of southeast Australia. Aust. J. Earth Sci. 55 (8), 1009–1021.
Crawford, J., Hughes, C.E., Lykoudis, S., 2014. Alternative least squares methods for determining the meteoric water line, demonstrated using GNIP data. J. Hydrol. 519, 2331–2340.
Crosbie, R.S., McCallum, J.L., Walker, G.R., Chiew, F.H., 2012. Episodic recharge and climate change in the Murray-Darling Basin, Australia. Hydrogeol. J. 20 (2), 245–261.
Cuthbert, M.O., Gleeson, T., Moosdorf, N., Befus, K.M., Schneider, A., Hartmann, J., Lehner, B., 2019. Global patterns and dynamics of climate–groundwater interactions. Nat. Clim. Chang. 9, 137–141.
Delworth, T.L., Zeng, F., 2014. Regional rainfall decline in Australia attributed to anthropogenic greenhouse gases and ozone levels. Nat. Geosci. 7, 583–587.
Edward, D., Watson, J., 1959. Fresh water and brackish water swamps of Rottnest Island. J. R. Soc. West. Aust. 42, 85–86.
Eliot, I., Clarke, D., 1986. Minor storm impact on the beachface of a sheltered sandy beach. Mar. Geol. 73 (1–2), 61–83.
Evans, A.D., Bennett, J.M., Ewenz, C.M., 2009. South Australian rainfall variability and climate extremes. Clim. Dyn. 33 (4), 477–493.
Farquhar, G.D., Cernusak, L.A., Barnes, B., 2007. Heavy water fractionation during transpiration. Plant Physiol. 143 (1), 11–18.
Ferguson, G., Gleeson, T., 2012. Vulnerability of coastal aquifers to groundwater use and climate change. Nat. Clim. Chang. 2, 342.
Hearty, P.J., 2003. Stratigraphy and timing of eolianite deposition on rottnest island, western Australia. Quat. Res. 60 (2), 211–222.
Hearty, P.J., O'Leary, M.J., 2008. Carbonate eolianites, quartz sands, and Quaternary sea-level cycles, Western Australia: a chronostratigraphic approach. Quat. Geochronol. 3 (1), 26–55.
Hollins, S.E., Hughes, C.E., Crawford, J., Cendón, D.I., Meredith, K.M., 2018. Rainfall isotope variations over the Australian continent – implications for hydrology and isoscape applications. Sci. Total Environ. 645, 630–645.
Houben, G.J., Koeniger, P., Sültenfuß, J., 2014. Freshwater lenses as archive of climate, groundwater recharge, and hydrochemical evolution: insights from depth-specific water isotope analysis and age determination on the island of Langeoog, Germany. Water Resour. Res. 50 (10), 8227–8239.
IAEA/WMO, 2016. Global Network of Isotopes in Precipitation. The GNIP Database.
Jiao, J., Post, V., 2019. Coastal Hydrogeology. Cambridge University Press, Cambridge, p. 403.
Jones, I.C., Banner, J.L., 2003. Estimating recharge thresholds in tropical karst island aquifers: Barbados, Puerto Rico and Guam. J. Hydrol. 278, 131–143.
Jurgens, B.C., Böhlke, J., Eberts, S.M., 2012. TracerLPM (Version 1): an Excel® Workbook for Interpreting Groundwater Age Distributions from Environmental Tracer Data, Techniques and Methods Report 4-F3. US Geological Survey, p. 60.
Katz, B., McBride, W., Hunt, A., Crandall, C., Metz, P., Eberts, S., Berndt, M., 2009. Vulnerability of a public supply well in a karstic aquifer to contamination. Gr. Water 47 (3), 438–452.
Kinzelbach, W., Bauer, P., Siegfried, T., Brunner, P., 2003. Sustainable Groundwater Management-Problems and Scientific Tool. Institute for Hydromechanics and Water Resources Management, ETH Zurich, Switzerland, pp. 279–284.
Lipar, M., Webb, J.A., 2014. Middle–late Pleistocene and holocene chronostratigraphy and climate history of the Tamala limestone, cooloongup and safety bay sands, nambung national park, southwestern western Australia. Aust. J. Earth Sci. 61 (8), 1023–1039.
Long, A.J., Putnam, L.D., 2006. Translating CFC-based piston ages into probability density functions of ground-water age in karst. J. Hydrol. 330 (3), 735–747.
Mahmud, K., Mariethoz, G., Baker, A., Treble, P., Markowska, M., McGuire, E., 2016. Estimation of deep infiltration in unsaturated limestone environments using cave lidar and drip count data. Hydrol. Earth Syst. Sci. 20 (1), 359–373.
Maloszewski, P., Stichler, W., Zuber, A., Rank, D., 2002. Identifying the flow systems in a karstic-fissured-porous aquifer, the Schneealpe, Austria, by modelling of environmental 18O and 3H isotopes. J. Hydrol. 256, 48–59.
Mory, A.J., 1995. Geology of the Wedge Island 1:100.000 Sheet. Geological Survey of Western Australia, Perth.
Nagra, G., Treble, P.C., Andersen, M.S., Bajo, P., Hellstrom, J., Baker, A., 2017. Dating stalagmites in mediterranean climates using annual trace element cycles. Sci. Rep. 7 (1), 621.
Ng, G.H.C., McLaughlin, D., Entekhabi, D., Scanlon, B.R., 2010. Probabilistic analysis of the effects of climate change on groundwater recharge. Water Resour. Res. 46. W07502.
Nicholls, R.J., Wong, P.P., Burkett, V.R., Codignotto, J.O., Hay, J.E., McLean, R.F., Ragoonaden, S., Woodroffe, C.D., 2007. Coastal Systems and Low-Lying Areas. Cambridge University Press, Cambridge, UK, p. 987.
Nicolini, E., Rogers, K., Rakowski, D., 2016. Baseline geochemical characterisation of a vulnerable tropical karstic aquifer; Lifou, New Caledonia. J. Hydrol.: Reg. Stud. 5, 114–130.
Playford, P.E., 1997. In: Vacher, H.L., Quinn, T. (Eds.), Geology and Hydrogeology of Carbonate Islands. Elsevier Science, pp. 783–810.
Playford, P.E., Leech, R.E.J., 1977. Geology and Hydrology of Rottnest Island. Geological Survey of Western Australia.
Playford, P.E., Low, G.H., Cockbain, A.E., 1976. Geology of the Perth Basin, Western Australia. Geological Survey of Western Australia, Bulletin.
Post, V., 2005. Fresh and saline groundwater interaction in coastal aquifers: is our technology ready for the problems ahead? Hydrogeol. J. 13 (1), 120–123.
Post, V.E.A., Bosserelle, A.L., Galvis, S.C., Sinclair, P.J., Werner, A.D., 2018. On the resilience of small-island freshwater lenses: evidence of the long-term impacts of groundwater abstraction on Bonriki Island, Kiribati. J. Hydrol. 564, 133–148.
Raupach, M., Briggs, P., Haverd, V., King, E., Paget, M., Trudinger, C., 2009. Australian water availability Project (AWAP): CSIRO. In: Marine and Atmospheric Research Component: Final Report for Phase, vol. 3. Bureau of Meteorology and CSIRO, p. 67.
Raupach, M., Briggs, P., Haverd, V., King, E., Paget, M., Trudinger, C., 2012. Australian Water Availability Project. CSIRO Marine and Atmospheric Research, Canberra, Australia.
Röper, T., Kröger, K.F., Meyer, H., Sültenfuss, J., Greskowiak, J., Massmann, G., 2012. Groundwater ages, recharge conditions and hydrochemical evolution of a barrier island freshwater lens (Spiekeroog, Northern Germany). J. Hydrol. 454, 173–186.
Small, C., Nicholls, R.J., 2003. A global analysis of human settlement in coastal zones. J. Coast. Res. 19 (3), 584–599.
Smith, I., McIntosh, P., Ansell, T., Reason, C., McInnes, K., 2000. Southwest Western Australian winter rainfall and its association with Indian Ocean climate variability. Int. J. Climatol. 20 (15), 1913–1930.
Treble, P.C., Bradley, C., Wood, A., Baker, A., Jex, C.N., Fairchild, I.J., Gagan, M.K., Cowley, J., Azcurra, C., 2013. An isotopic and modelling study of flow paths and storage in Quaternary calcarenite, SW Australia: implications for speleothem paleoclimate records. Quat. Sci. Rev. 64, 90–103.
Treble, P.C., Fairchild, I.J., Baker, A., Meredith, K.T., Andersen, M.S., Salmon, S.U., Bradley, C., Wynn, P.M., Hankin, S.I., Wood, A., McGuire, E., 2016. Roles of forest bioproductivity, transpiration and fire in a nine-year record of cave dripwater chemistry from southwest Australia. Geochem. Cosmochim. Acta 184, 132–150.
Vogel, J., 1967. Investigation of Groundwater Flow with Radiocarbon. International Atomic Energy Agency, Vienna, pp. 355–369.
White, I., Falkland, T., 2010. Management of freshwater lenses on small Pacific islands. Hydrogeol. J. 18, 227–246.